Available online at www.sciencedirect.com
ScienceDirect
Journal of Catalysis 255 (2008) 144–152
JOURNAL OF CATALYSIS
www.elsevier.com/locate/jcat

"Ir-in-ceria": A highly selective catalyst for preferential CO oxidation

Yanqiang Huang [a,b], Aiqin Wang [a], Lin Li [a], Xiaodong Wang [a], Dangsheng Su [c], Tao Zhang [a,*]

[a] State Key Laboratory of Catalysis, Dalian Institute of Chemical Physics, Chinese Academy of Sciences, Dalian 116023, People's Republic of China
[b] Graduate University of Chinese Academy of Sciences, Beijing 100049, People's Republic of China
[c] Fritz-Haber-Institut der Max-Planck-Gesellschaft, Faradayweg 4-6, 14195 Berlin, Germany

Received 14 January 2008; accepted 24 January 2008

Available online 6 March 2008

Abstract

An Ir-in-ceria catalyst has been developed, in which most of the iridium particles are embedded in the ceria matrix through the redox reaction between Ce^{3+} and Ir^{4+}, which occurred during co-precipitation (CP). This Ir-CP catalyst exhibited high activity for preferential CO oxidation under excess hydrogen conditions, and the selectivity to CO_2 remained nearly constant, at around 70%, with increasing reaction temperature. Temperature-programmed reduction and in situ diffuse reflectance infrared spectroscopy techniques were used to explore the structure of the Ir-CP catalyst and to correlate it with the catalytic performance. It was found that the CeO_2 support was activated by iridium and formed on the surface the active sites for CO oxidation. Due to the absence of extensively exposed Ir species on the Ir-CP catalyst, H_2 oxidation occurring on the Ir species and the ceria support at high temperatures was significantly suppressed, thus keeping the selectivity to CO_2 at a high level.

Keywords: Preferential CO oxidation; Iridium; Ceria; Selectivity; Ir/CeO_2

1. Introduction

Polymer electrolyte membrane fuel cells (PEMFCs) operating with hydrogen have proven to be the most promising candidates for transport applications [1]. The PEMFCs operate at relatively low temperatures (~80–120 °C), and the anode catalysts are easily poisoned by even traces of CO. Traditional routes for hydrogen generation yield significant amounts of CO (ca. 5–15%) as the byproduct. A subsequent water–gas shift (WGS) reaction can reduce the CO amount to about 0.5–1% [2]. Thus, it is necessary to further reduce the amount of CO to about 10 ppm while minimizing the consumption of hydrogen. Several chemical and/or physical methods have been used to obtain a high purification level of the hydrogen fuel. Among these alternatives, preferential oxidation of CO under excess hydrogen conditions (PROX) seems to be a promising process [3,4].

To date, various catalytic formulations have been investigated in the PROX reaction. In particular, ceria-supported noble metal (NM) catalysts exhibited better performance in the range of 90–130 °C compared with alumina-supported ones [5–10]. A noncompetitive Langmuir–Hinshelwood mechanism has been proposed to be responsible for the high activities of the NM/CeO_2, in which the CO adsorbed on the NM reacts with the oxygen activated on the ceria support. This mechanism involves the direct participation of the NM, which provides sites for CO adsorption. Nevertheless, there is currently an ongoing debate about the role of NM in these ceria-containing samples. Hardacre et al. [11] observed enhanced rates of CO oxidation on a Pt (111) single crystal encapsulated by ceria. Similarly, Golunski et al. [12–14] found that the addition of the NM led to a dramatic increase in the number of oxygen vacancies within the ceria, which became active sites for CO oxidation. Recently, Deng et al. [15] reported that Au/CeO_2 catalysts can be effective for the PROX reaction even after removal of the neutral Au clusters. In these examples, the activated ceria support, without direct participation of the NM, can act as the active sites for CO oxidation. A similar phenomenon also was found in the WGS reaction; for example, the rate of the WGS reaction remained the same when the metallic NM was removed [16] or encapsulated in the ceria [17,18].

* Corresponding author. Fax: +86 411 84691570.
E-mail address: taozhang@dicp.ac.cn (T. Zhang).

0021-9517/$ – see front matter
doi:10.1016/j.jcat.2008.01.024

Motivated by these experimental findings, we attempted to design a highly selective PROX catalyst, in which the CO oxidation reaction can proceed on the activated ceria surface alone while the H_2 oxidation occurring on the metal sites is significantly suppressed. Toward this goal, we prepared an Ir-in-ceria catalyst (with most of the Ir particles embedded in the ceria) using co-precipitation (CP), as reported by Rajaram et al. [19]. The Ir-in-ceria was chosen due to the fact that Ir has been less widely explored than Pt or Au, and also because Ir/CeO_2 can be as active as Pt/CeO_2 for the PROX reaction [20]. For comparison, an Ir-on-ceria catalyst (with the Ir particles deposited mainly on the ceria surface) also was prepared by deposition–precipitation (DP). It was found that the difference in the structures of these two catalysts affected their catalytic performance, especially in terms of selectivity behavior. Thus, the present work provides an example of a structure–reactivity relationship.

2. Experimental

2.1. Catalyst preparation

To prepare the Ir-in-ceria catalyst, an aqueous solution of H_2IrCl_6 and $Ce(NO_3)_3$ was added to a heated NaOH solution (80 °C) to form a black precipitate, as described previously [19]. After aging for 2 h, the suspension was filtered and washed with deionized water several times. Then the solid material was dried at 60 °C overnight and finally calcined at 400 °C for 2 h. The resultant samples, designated Ir-CP, had Ir metal loadings ranging from 0.20 to 5.00 wt%. For comparison, Au-CeO_2 and Pt-CeO_2 catalysts with 1.60 wt% of metal also were prepared under the same conditions and designated Au-CP-1.60 wt% and Pt-CP-1.60 wt%. To study the effect of the synthesis parameters on the properties of the resultant catalysts, we used various precipitants (urea, Na_2CO_3, and NaOH) and precipitation temperatures (ranging from 20 to 100 °C). The resultant samples are designated Ir-CP-X, where X represents the precipitant (in which case, with the precipitation temperature fixed at 80 °C) or the precipitation temperature (in which case, NaOH was always used as the precipitant).

The Ir-on-ceria catalyst was prepared by the conventional DP procedure, where the ceria support was suspended in an aqueous solution of H_2IrCl_6 and the pH was adjusted to 8–9 using NaOH as the neutralizer. After the same drying and calcining treatments as for the Ir-CP catalyst, the catalyst, designated Ir-DP, was obtained. The ceria support was prepared by precipitation from $Ce(NO_3)_3$ under preparation conditions similar to those used for the Ir-CP catalyst.

2.2. Activity test

Catalytic performance was evaluated in a fixed-bed flow reactor at atmospheric pressure using 100 mg of a catalyst diluted with SiC. Before the test, the catalyst was reduced in situ with hydrogen at 400 °C for 2 h. After cooling to room temperature, a reacting gas containing 2 vol% CO, 1 vol% O_2, and 40 vol% H_2 in He was allowed to pass through the reactor at a flow rate of 67 $cm^3\,min^{-1}$ (STP), corresponding to a space velocity of 40,000 $mL\,h^{-1}\,g_{Cat}^{-1}$. In some cases, a feed stream composed of 2 vol% CO and 1 vol% O_2 with He balance was used to evaluate the activity for CO oxidation. H_2O was introduced into the system by passing the stream through a saturator to create the required H_2O concentration. The effluent gas was analyzed using an online gas chromatograph system (Angilent GC-8800) equipped with a thermal conductivity detector. CO_2 and H_2O were detected as the only products. No methane was found under our experimental conditions.

CO conversion (X_{CO}) is calculated as

$$X_{CO} = \frac{n_{CO}^{in} - n_{CO}^{out}}{n_{CO}^{in}} \times 100(\%). \tag{1}$$

Selectivity (S) to CO_2 is defined as the ratio of the oxygen transformed into CO_2 to the total oxygen consumed:

$$S = \frac{n_{CO_2}^{out}}{2(n_{O_2}^{in} - n_{O_2}^{out})} \times 100(\%). \tag{2}$$

The relation between conversion and selectivity is defined as

$$X_{CO} = \frac{S X_{O_2}}{100}\lambda(\%), \tag{3}$$

where λ is the oxygen excess factor, by definition,

$$\lambda = \frac{2n_{O_2}^{in}}{n_{CO}^{in}}. \tag{4}$$

2.3. Characterization

Brunauer–Emmett–Teller (BET) surface areas of the catalysts were measured by nitrogen adsorption at −196 °C using a Micromeritics ASAP 2010 apparatus. The actual Ir loadings of the catalysts were determined by inductively coupled plasma (ICP) analysis, and the chlorine residues in the catalysts were determined by X-ray fluorescence (XRF). Powder X-ray diffraction (XRD) patterns were obtained with a Rigaku (D/MAX-βB) diffractometer equipped with an online computer.

Temperature-programmed reduction (TPR) experiments were carried out on a Micromeritics AutoChem II 2920 Automated Catalyst Characterization System. First, 100 mg of a catalyst was loaded into a U-shape quartz reactor and pretreated with air at 400 °C for 1 h to remove adsorbed carbonates and hydrates. Then, after cooling to room temperature, the flowing gas was switched to a 10 vol% H_2/Ar, and the catalyst was heated to 900 °C at a ramping rate of 10 °C min^{-1}.

In situ diffuse reflectance infrared spectroscopy (DRIFTS) spectra were acquired with a BRUKER Equinox 55 spectrometer, equipped with a MCT detector and operated at a resolution of 4 cm^{-1}. Before each experiment, a 40-mg sample in a powder form was reduced in situ with H_2 at 400 °C for 2 h. After cooling to 100 °C, the gas for adsorption (CO alone or a PROX reaction mixture) was introduced into the reaction cell at a total flow rate of 100 mL min^{-1} (GHSV = 120,000 $mL\,h^{-1}\,g_{Cat}^{-1}$). The spectra were recorded as a function of the time on stream for 60 min in all cases, against a background of the sample at the reaction temperature under flowing He. All spectra were obtained under steady-state conditions.

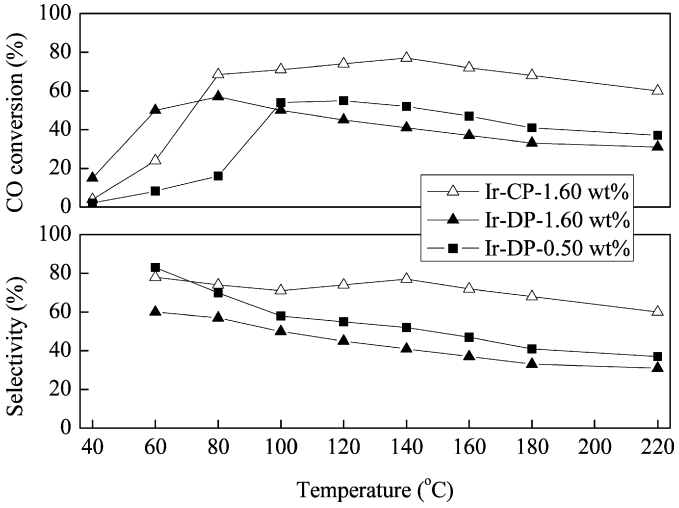

Fig. 1. CO conversion and selectivity to CO_2 as a function of reaction temperature in the PROX reaction over 100 mg of the Ir-CP-1.60 wt% (△), Ir-DP-1.60 wt% (▲) and Ir-DP-0.50 wt% (■) catalysts. Reacting gas composition: $CO/O_2/He/H_2 = 2/1/57/40$ (vol%); GHSV = 40,000 mL h^{-1} g_{Cat}^{-1}.

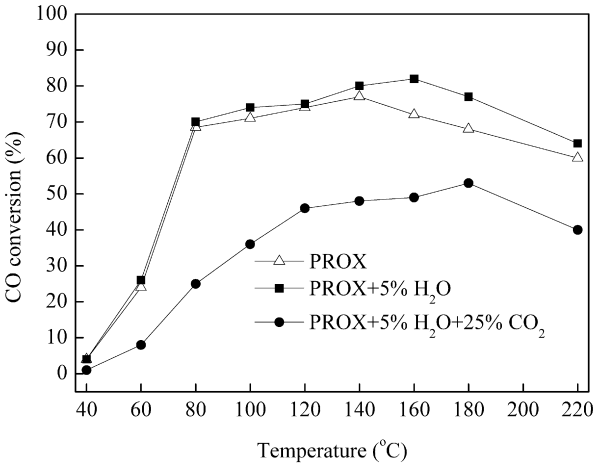

Fig. 2. CO conversion as a function of reaction temperature over the Ir-CP-1.60 wt% in the presence of 5% H_2O (■), both 5% H_2O and 25% CO_2 (●), and none of them (△).

3. Results

3.1. Activity test

Fig. 1 illustrates CO conversion and selectivity to CO_2 on both Ir-DP-1.60 wt% and Ir-CP-1.60 wt% samples. Note that at low temperatures (<80 °C), the Ir-DP-1.60 wt% catalyst was more active than the Ir-CP-1.60 wt%; however, above 80 °C, the Ir-CP-1.60 wt% showed higher CO oxidation activity than the Ir-DP-1.60 wt%. More importantly, the Ir-CP-1.60 wt% exhibited high selectivity to CO_2 in the PROX reaction. The selectivity to CO_2 remained nearly constant, at around 70%, with increasing reaction temperature from 80 to 180 °C. In contrast, over the Ir-DP-1.60 wt%, the selectivity decreased from 57% at 80 °C to only 33% at 180 °C. Clearly, as desired, the Ir-CP sample exhibited a wider temperature window to give a high selectivity to CO_2 and appeared to be more promising for the PROX reaction. Because the Ir-CP was designed to have an Ir-in-ceria structure, whereas the Ir-DP has an Ir-on-ceria structure, it is reasonable to speculate that the difference in catalytic performance between the Ir-CP and Ir-DP samples was due to the difference in the number of the Ir sites exposed on the ceria support surface. To confirm this, we reduced the metal loading on the Ir-DP sample to 0.50 wt%, and found that this Ir-DP-0.50 wt% sample exhibited higher selectivity than the Ir-DP-1.60 wt% sample, although it had much lower activity below 100 °C.

The effects of H_2O and/or CO_2 on CO oxidation behavior over the Ir-CP-1.60 wt% catalyst are shown in Fig. 2. The presence of 5% H_2O in the feed stream seemed to be slightly favorable to the catalytic activity, especially at relatively high temperatures. Similar results also were obtained on other ceria-based catalysts [15,21]. A possible explanation for this finding is that the presence of water accelerated the WGS reaction, and thus more CO was converted into CO_2. A time-on-stream test under the presence of 5% H_2O showed that the Ir-CP-1.60 wt% catalyst had good stability; CO conversion at 100 °C remained constant at around 68% over 10 h. On the other hand, addition of 25% CO_2 led to a significant decrease in CO conversion, which may be associated with carbonate deposition. This deactivation process became less prominent at high temperatures due to the decomposition of carbonate species.

For the CP process, the precipitant and precipitation temperature were important parameters affecting the catalytic performance of the resultant catalysts (Table 1). We investigated the effect of precipitant using different bases (Na_2CO_3, urea, and NaOH) as the precipitants, while keeping the precipitation temperature at 80 °C. The CO conversions on the Ir-CP-NaOH were higher than those on the Ir-CP-urea, which in turn were higher than those on the Ir-CP-Na_2CO_3. Thus, it seems that the activities of the resultant Ir-CP catalysts for CO oxidation are related to the base strength of the precipitants used. Clearly, NaOH was the preferred base precipitant in our case.

Choosing NaOH as the most suitable precipitant, we investigated the effect of precipitation temperature (Table 1). CO conversion at 80 °C was used as an index for the activity, whereas that at 180 °C was regarded as an indicator for the selectivity to CO_2. When CP was carried out at 20 °C, the resulting Ir-CP-20 °C exhibited a very poor activity for CO oxidation. Increasing the precipitation temperature from 20 to 80 °C resulted in enhanced activity. For example, when precipitation was carried out at 80 °C, the CO conversion at 80 °C was similar to that at 180 °C, indicating that the catalyst was both highly active and selective. However, on a further increase in precipitation temperature from 80 to 100 °C, CO conversion at 80 °C remained high, but conversion at 180 °C decreased. This indicates that the selectivity to CO_2 decreased when the catalyst was prepared at a precipitation temperature above 80 °C. From the foregoing results, it can be concluded that the best precipitation temperature was 80 °C.

Besides the precipitation parameters, the Ir loading also exerted a significant effect on the catalytic performance for CO oxidation (also Table 1). On increasing metal content from 0.20 to 1.60 wt%, the CO conversion at 80 °C increased from 3

Table 1
Activity data for the PROX reaction on the Ir-CP-X catalysts at a reaction temperature of 80, 140, and 180 °C

Catalysts Ir-CP-X	80 °C		140 °C		180 °C		TOF ($\times 10^{-3}$ s^{-1})[c]
	X_{CO} (%)[a]	X_{O_2} (%)[b]	X_{CO} (%)	X_{O_2} (%)	X_{CO} (%)	X_{O_2} (%)	
X: precipitant							
Ir-CP-Na_2CO_3	1	4	3	25	14	100	0.8
Ir-CP-urea	29	40	44	100	35	100	4.1
Ir-CP-NaOH	68	92	77	100	68	100	10.1
X: precipitation temperature							
Ir-CP-20 °C	7	8	13	18	43	97	1.6
Ir-CP-40 °C	26	33	67	100	68	100	2.9
Ir-CP-60 °C	54	71	71	100	68	100	7.2
Ir-CP-80 °C	68	92	77	100	68	100	10.1
Ir-CP-100 °C	68	100	54	100	54	100	13.0
X: Ir loading							
Ir-CP-0.20 wt%	3	4	28	36	65	100	0.6
Ir-CP-0.50 wt%	22	28	67	100	67	100	2.7
Ir-CP-1.00 wt%	34	39	71	100	68	100	5.7
Ir-CP-1.60 wt%	68	92	77	100	68	100	10.1
Ir-CP-5.00 wt%	52	100	38	100	33	100	21.4

[a] X_{CO} = CO conversion.
[b] X_{O_2} = O_2 conversion.
[c] The TOFs of CO oxidation were calculated on the basis of the amount of reducible oxygen on the surface as measured by H_2-TPR; test condition: 2% CO–1% O_2–40% H_2–He; temperature: 100 °C.

to 68%, but the CO conversion at 180 °C remained constant (around 68%). However, the Ir-CP-5.00 wt% sample exhibited low CO conversions at both 80 and 180 °C, possibly due to competitive H_2 oxidation. Thus, there appears to be an optimum metal loading for the Ir-CP samples, with the best results found on the catalyst containing 1.60 wt% iridium. Consequently, we chose the Ir-DP and Ir-CP samples with a nominal metal loading of 1.60 wt% for further characterization studies.

3.2. Routine determinations

The BET surface areas of the Ir-CP-1.60 wt% and Ir-DP-1.60 wt% were 120 and 106 m^2 g^{-1}, respectively. The Ir loadings on the two catalyst samples, as determined by ICP, were similar (1.50 wt% for the Ir-CP-1.60 wt% and 1.47 wt% for the Ir-DP-1.60 wt%); however, the surface Ir/Ce atomic ratio on the Ir-CP-1.60 wt% sample, determined by XPS analysis, was significantly lower than that on the Ir-DP-1.60 wt% (0.0035 vs 0.0091). This implies that most of the Ir particles on the Ir-CP-1.60 wt% are embedded in the ceria matrix, in accordance with the Ir-in-ceria structure. No Cl residues were detected by XRF analysis in either sample. XRD patterns of the Ir-CP-1.60 wt% and Ir-DP-1.60 wt% were similar (results not shown). Only those diffraction peaks corresponding to crystalline CeO_2 were observed, and neither an IrO_2 nor an Ir phase was detected, irrespective of preparation method. This is likely due to the very small sizes of the Ir particles in both samples; CeO_2 particle sizes were estimated to be ~6 nm according to the Debye–Scherrer equation, as confirmed by HRTEM. Thus, the Ir-CP-1.60 wt% and Ir-DP-1.60 wt% had similar metal loadings, similar support particle sizes, and complete removal of chlorine, which allowed us to analyze the difference in their catalytic performance without the need to consider these parameters [6,20].

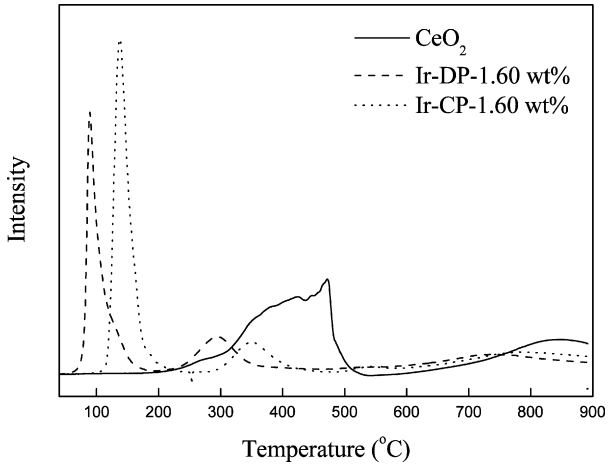

Fig. 3. H_2-TPR profiles of ceria, Ir-CP-1.60 wt% and Ir-DP-1.60 wt% samples.

3.3. H_2 TPR

The H_2-TPR technique is often used to characterize ceria-supported catalysts, because it can provide useful information on the generation of oxygen vacancies as well as on metal–support interactions. The H_2-TPR profiles of CeO_2, Ir-CP-1.60 wt% and Ir-DP-1.60 wt% are shown in Fig. 3. The TPR profile of CeO_2 presented two reduction peaks. The broad peak at around 480 °C was assigned to the reduction of surface oxygen, whereas the peak at around 800 °C was due to bulk ceria reduction [22,23]. In agreement with previous studies [20,24,25], the loading of iridium had no affect on the reduction of bulk ceria, but effectively promoted the reduction of surface

Table 2
Reducibility of Ir/CeO_2 catalysts and ceria support as measured by H_2-TPR

Sample	H_2 consumed (μmol g_{Cat}^{-1})	
	Peak 1 (T)	Peak 2 (T)
CeO_2		1160 (470 °C)
Ir-DP-1.60 wt%	937 (89 °C)	223 (295 °C)
Ir-CP-1.60 wt%	1071 (140 °C)	178 (350 °C)

oxygen on ceria, associated with a new signal appearing at low temperatures. The peak temperatures and corresponding hydrogen consumptions are listed in Table 2.

For the Ir-DP-1.60 wt% sample, the major reduction peak at around 90 °C should be an overlap profile of the reduction of the Ir^{4+} species and the most easily reducible CeO_2, because the amount of H_2 consumed (~937 μmol g_{Cat}^{-1}) greatly exceeded that required for the reduction of iridium oxide. (The calculated amount of hydrogen consumed for reducing Ir^{4+} to metallic Ir is only 150 μmol g_{Cat}^{-1}.) In addition, the reduction peak at about 300 °C would be due to the reduction of surface CeO_2, which has no strong interaction with iridium [19,24]. The Ir-CP-1.60 wt% sample showed an initial reduction peak at about 140 °C, 50 °C higher than that of the Ir-DP-1.60 wt% sample. This lower reduction temperature should be related to the Ir-DP-1.60 wt% sample's slightly higher activity at low temperatures (Fig. 1). Moreover, the hydrogen consumption corresponding to the first peak was greater for Ir-CP-1.60 wt% than for Ir-DP-1.60 wt%, leading to more oxygen vacancies on the former catalyst. As described previously [19], the NM in a NM/CeO_2-CP catalyst exists mainly in a metallic state, regardless of the thermal treatment. Moreover, the NM species are mostly blocked within the internal surface of the solid. Thus, we can speculate that the first reduction peak of the Ir-CP-1.60 wt% should be mainly associated with the reduction of surface oxygen of CeO_2. Our observations seem to be consistent with the idea of a "junction effect" [26] arising from the contact between ceria and a metal with a high work function.

From the foregoing results, we can postulate that the activated ceria can be easily reduced at low temperatures, and thus be responsible for the creation of oxygen vacancies. Oxygen vacancies are known to be chemically active and play an important role in low-temperature CO oxidation [27–29]. Accordingly, we characterized the Ir-CP catalysts with different precipitants and precipitation temperatures, as well as with various Ir loadings, giving special attention to their low-temperature reduction peaks (Table 3). Varying the precipitant from Na_2CO_3, urea to NaOH, the amount of hydrogen consumed for the Ir-CP samples increased from 750, to 892, and then to 1071 μmol g_{Cat}^{-1}. In addition, both the Ir loading and the precipitation temperature had a significant affect on the reducibility of the ceria support. A higher precipitation temperature or a higher Ir loading resulted in higher H_2 consumption and a lower reduction temperature. Comparing the H_2 consumption (Table 3) with the activity level (Table 1) demonstrates a direct correlation between the reducibility of the surface ceria and its catalytic activity for CO oxidation. Higher hydrogen consumption often was observed on the highly active samples.

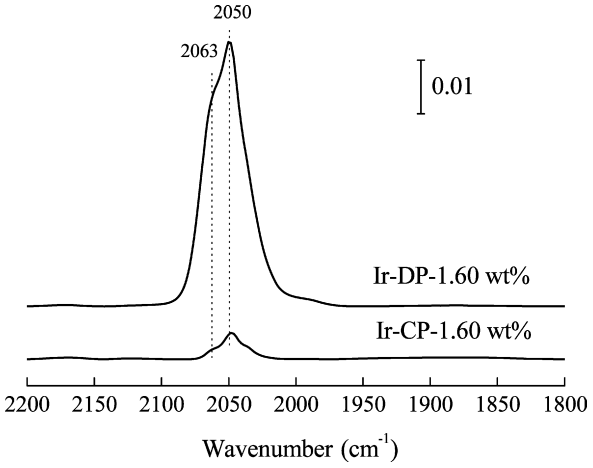

Fig. 4. Typical DRIFTS spectra of Ir-CP-1.60 wt% and Ir-DP-1.60 wt% samples obtained under steady-state CO adsorption conditions at 100 °C.

3.4. In situ DRIFTS

To further verify whether the Ir particles in the Ir-CP sample were embedded in the ceria matrix, as desired, we investigated the CO adsorption behavior over the Ir-CP-1.60 wt% at 100 °C using in situ DRIFTS. For comparison, we also performed the same experiments on the Ir-DP-1.60 wt% catalyst. As shown in Fig. 4, CO adsorption on the Ir-DP-1.60 wt% sample produced a strong band at 2050 cm^{-1} and a shoulder at 2063 cm^{-1}, which can be attributed to CO species linearly adsorbed on the different Ir^0 sites [30–32]. In contrast, CO adsorption on the Ir-CP-1.60 wt% sample yielded only a very weak band of at least 10-fold lower intensity than that on the Ir-DP-1.60 wt% sample. This result strongly suggests that most of the Ir particles

Table 3
Reducibility of the Ir-CP-X catalysts as measured by H_2-TPR

Precipitants		Metal loadings		Precipitation temperatures	
Sample	H_2 consumed (μmol g_{Cat}^{-1})	Sample	H_2 consumed (μmol g_{Cat}^{-1})	Sample	H_2 consumed (μmol g_{Cat}^{-1})
Ir-CP-Na_2CO_3	750 (147 °C)[a]	Ir-CP-0.20 wt%	830 (197 °C)	Ir-CP-20 °C	580 (183 °C)
		Ir-CP-0.50 wt%	915 (182 °C)	Ir-CP-40 °C	758 (145 °C)
Ir-CP-urea	892 (140 °C)	Ir-CP-1.00 wt%	973 (150 °C)	Ir-CP-60 °C	803 (141 °C)
		Ir-CP-1.60 wt%	1071 (140 °C)	Ir-CP-80 °C	1071 (140 °C)
Ir-CP-NaOH	1071 (140 °C)	Ir-CP-5.00 wt%	1343 (117 °C)	Ir-CP-100 °C	1116 (136 °C)

[a] The number in brackets indicates the first reduction peak temperature.

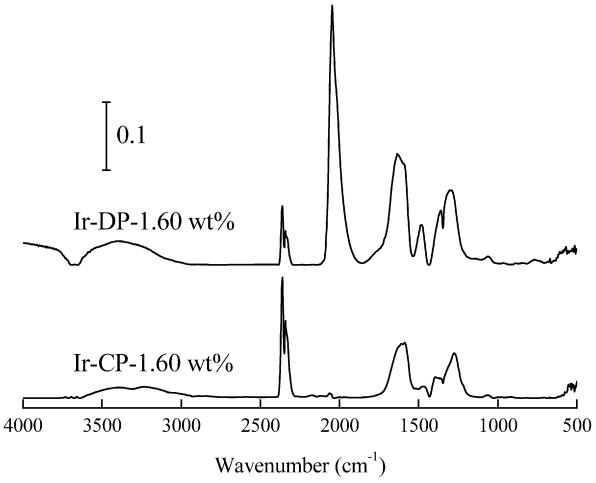

Fig. 5. Typical DRIFTS spectra of Ir-CP-1.60 wt% and Ir-DP-1.60 wt% samples obtained under steady-state PROX conditions at 100 °C.

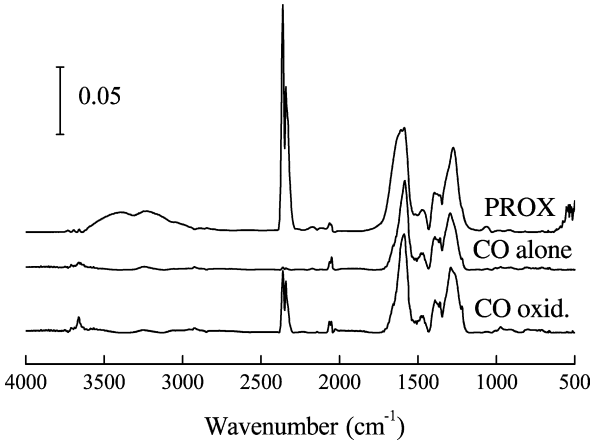

Fig. 6. Typical DRIFTS spectra of Ir-CP-1.60 wt% sample obtained under different steady-state conditions at 100 °C.

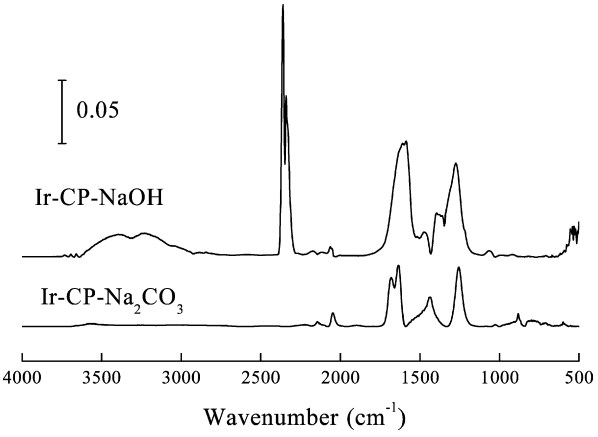

Fig. 7. Typical DRIFTS spectra of Ir-CP-NaOH and Ir-CP-Na_2CO_3 samples obtained under steady-state PROX conditions at 100 °C.

in the Ir-CP-1.60 wt% sample were embedded in the ceria support, whereas those on the Ir-DP-1.60 wt% sample were mainly exposed on the ceria surface.

Fig. 5 compares the DRIFTS spectra on the Ir-CP-1.60 wt% and Ir-DP-1.60 wt% samples during the PROX reaction at 100 °C. The bands in the 1700–1200 cm^{-1} region can be ascribed to different carbonates [7,8,18,33,34]. The broad bands centered at 3421 cm^{-1} are assigned to hydrogen-bonded adsorbed water on the ceria surface [7,8], whereas the bands at around 2360 cm^{-1} are associated with gas-phase CO_2. Comparing the spectra on the two catalysts raises some interesting points. First, the main difference between them concerns the strength of the CO adsorption band. The low intensity of the CO adsorption band on the Ir-CP-1.60 wt% should relate to the Ir-in-ceria structure. Second, the band for gas-phase CO_2 was stronger on Ir-CP-1.60 wt% than on Ir-DP-1.60 wt%, indicating greater CO oxidation activity on the former. Third, the bands attributed to hydrogen-bonded water (centered at 3421 cm^{-1}) were stronger on Ir-DP-1.60 wt% than on Ir-CP-1.60 wt%, suggesting greater H_2 oxidation activity on the former, in agreement with the H_2-TPR findings. In addition, we found that CO formed several carbonates by reacting with the surface oxygen on both samples, and the intensity of these species was greater on Ir-DP-1.60 wt% than on Ir-CP-1.60 wt%.

The DRIFTS spectra on the Ir-CP-1.60 wt% recorded under different reaction environments (PROX mixture, CO alone, and CO oxidation) are shown in Fig. 6. Initially, the spectra were collected under the PROX condition after a steady-state condition was established; later, the H_2 and O_2 were removed from the stream. In this case, the gas-phase CO_2 bands disappeared quickly, along with the hydrogen-bonded adsorbed water. Subsequently, oxygen was introduced to the stream. The gas-phase CO_2 band reappeared, but was smaller than that under the PROX condition, implying a lower activity level in the absence of H_2.

The DRIFTS spectra collected on Ir-CP-Na_2CO_3 (a nonactive catalyst) and Ir-CP-NaOH (a highly active catalyst) under the PROX condition at 100 °C are compared in Fig. 7. The carbonyl species were very weak on both samples, implying that the CP procedure could yield an Ir-in-ceria structure regardless of whether NaOH or Na_2CO_3 was used as the precipitant. In contrast to the appearance of a stronger band for gas-phase CO_2 on the Ir-CP-NaOH, neither CO_2 nor H_2O was detected on the Ir-CP-Na_2CO_3 sample. These observations are consistent with the results obtained in the catalytic reactor tests. Moreover, the stretching vibration bands at 1700–1200 cm^{-1} were relatively weak on the Ir-CP-Na_2CO_3. Considering that such species are generally formed on activated ceria supports [34], we thus can propose that the ceria on the Ir-CP-Na_2CO_3 was not sufficiently activated to form extensive oxygen vacancies.

4. Discussion

An effective PROX catalyst should have a wide operation window to avoid the need for precise temperature control. However, in most cases, the selectivity to CO_2 tends to decrease with increasing reaction temperature due to the competitive oxidation of H_2. To address this problem, we prepared a highly selective ceria-supported iridium catalyst with a special Ir-in-ceria structure (as revealed by the DRIFTS spectra in Figs. 4 and 5), on which H_2 oxidation on the metallic Ir sites can be

significantly suppressed. In contrast, the Ir-DP-1.60 wt% sample unambiguously exhibited an Ir-on-ceria structure. The different structures of the Ir-CP-1.60 wt% and Ir-DP-1.60 wt% determined their different behaviors in the PROX reaction, especially in terms of selectivity to CO_2. The Ir-CP-1.60 wt% sample exhibited high CO oxidation activity in the PROX reaction and almost no loss in selectivity in the temperature range 80–180 °C, whereas the Ir-DP-1.60 wt% catalyst, due to its high H_2 oxidation activity, demonstrated a continuous drop in selectivity.

To gain insight into this structure–reactivity relationship, we changed precipitants from NaOH to Na_2CO_3 and compared the catalytic performance of the resultant catalysts. Fig. 7 and Table 1 clearly show that the Ir-CP-Na_2CO_3 sample exhibited very poor activity and selectivity even though it also had an Ir-in-ceria structure. This unexpected result reminds us that the metal-in-ceria structure is not the only factor determining catalytic performance; some other intrinsic factors must be affecting the activity and selectivity of the Ir-CP catalyst. Considering the several preparation parameters that influence catalytic performance (Table 1), we believed that analyzing the interaction between Ir and ceria during the preparation process would help us uncover those unknown factors in the Ir-in-ceria structure that are actually responsible for the high selectivity to CO_2.

It is well known that Ce^{3+} can be oxidized to form Ce^{4+} hydroxyl species in alkaline environments and in the presence of oxygen [19,35,36]. In a basic solution, the redox potential can be quantified by the equation $E_{Ce(4+)/Ce(3+)} = [0.787 - 0.0592^*pH]$ V [37], corresponding to K_{sp} values of 1.6×10^{-20} and 2.5×10^{-47} for $Ce(OH)_3$ and $Ce(OH)_4$, respectively. A decrease in emf will occur with increasing the pH, thus facilitating the oxidation of Ce^{3+} to Ce^{4+}; however, the reaction is thermodynamically unfavorable due to the high emf. On the other hand, if CeO_2 were formed instead of $Ce(OH)_4$, then oxidation would be strongly favored due to its very low K_{sp} (1.25×10^{-63}). In that case, the redox potential can be quantified by the equation $E_{Ce(4+)/Ce(3+)} = [-0.112 - 0.0592^*pH]$ V [37]. In this CP process, the oxidation of Ce^{3+} to Ce^{4+} is coupled with the reduction of Ir^{4+} to Ir^0. Our XRD examination of the as-synthesized (uncalcined) Ir-CP catalysts revealed the formation of a phase-pure CeO_2. Moreover, the black color of the as-synthesized Ir-CP (compared with the green-colored Ir-DP) also is indicative of the metallic state of iridium. Therefore, the key to this coupled redox process is the formation of CeO_2 in solution, which is favored under strongly basic conditions and at high temperatures [38].

This redox-precipitation procedure, besides the formation of an Ir-in-ceria structure, induces strong, extensive interactions between Ir and ceria. The metal–support interactions can be roughly quantified by the reducibility of the surface ceria promoted by iridium. Fig. 8 plots the CO conversions at 80 °C (Table 1) versus the amount of H_2 consumed for surface ceria reduction (Table 3). The clear strongly positive correlation between them implies that oxygen vacancies on the ceria surface, formed with the aid of iridium, may act as the active sites in this reaction [12–14]. Consequently, we calculated turnover frequencies (TOFs) of CO oxidation on the basis of the amount of

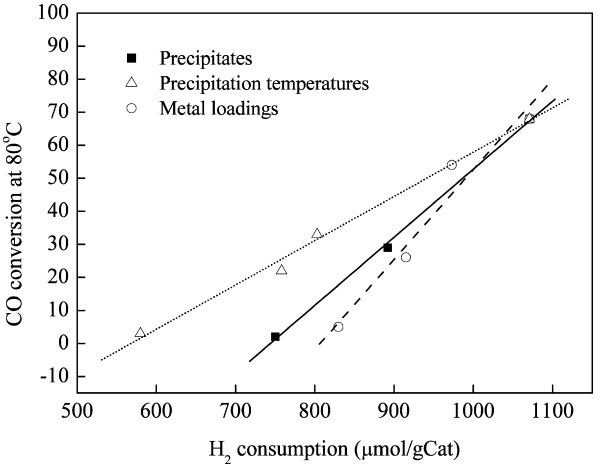

Fig. 8. CO conversions at 80 °C plot for the hydrogen consumed for the surface CeO_2 reduction over the Ir-in-ceria catalysts. The scatters are experimental data. The lines are obtained by linear fitting.

reducible oxygen on the surface as measured by H_2-TPR [15]. Although this calculation may underestimate the TOF values by considering that not all of the surface oxygen vacancies participate in the reaction, it can help us better understand the reaction on the different Ir-CP catalysts. As shown in Table 1, the TOFs increased with increasing base strength, precipitation temperature, and Ir loading. When the precipitation proceeded under a less strongly basic environment (such as with urea or Na_2CO_3) or at a lower temperature (below 80 °C), the redox reaction between Ce^{3+} and Ir^{4+} occurred to a lesser extent or did not occur at all. In such cases, the interaction between Ir and ceria was not strong enough to activate the surface ceria, resulting in lower activity. In contrast, when the precipitation was conducted at a higher temperature or more Ir species were incorporated into the ceria support, as in the case of Ir-CP-100 °C and Ir-CP-5.00 wt%, a stronger interaction between Ir and ceria was seen. In these cases, the ceria was overactivated, and the resulting Ir-CP catalysts were more active for the undesired H_2 oxidation reaction as well, leading to decreased CO conversion and selectivity to CO_2 [39]. This finding demonstrates that the ceria support must be properly activated to obtain the desired selectivity to CO_2.

For comparison, we also calculated the TOF on Ir-DP-1.60 wt% on the basis of the reducible oxygen atoms, and found it to be slightly higher than that on the Ir-CP-1.60 wt% catalyst (Table 4). But if the extensively exposed Ir sites on the Ir-DP-1.60 wt% were considered the active sites for CO oxidation and the dispersion was assumed to be 100%, then its TOF value ($0.184\ s^{-1}$) was one order of magnitude greater than that on the Ir-CP-1.60 wt% catalyst ($0.010\ s^{-1}$). Such a high activity level of the Ir-DP-1.60 wt% would cause undesirable H_2 oxidation and thereby decrease the selectivity to CO_2.

Because Au/CeO_2 and Pt/CeO_2 have been extensively studied for the PROX reaction [5–10,15], we prepared Au-CP-1.60 wt% and Pt-CP-1.60 wt% catalysts under the same precipitation conditions and evaluated their catalytic performance for the PROX reaction in comparison with Ir-CP-1.60 wt%. The selectivities of these catalysts at 100 and 180 °C, as well as their

Table 4
Comparison of reducibility, TOFs of CO oxidation, and selectivity to CO_2

Catalyst	H_2 consumed ($\mu mol\ g_{Cat}^{-1}$)	Selectivity to CO_2		TOF ($\times 10^{-3}\ s^{-1}$)[b]
		100 °C	180 °C	
Ir-DP-1.60 wt%	937 (89 °C)[a]	54	33	14.0
Ir-CP-1.60 wt%	1071 (140 °C)	71	68	10.1
Pt-CP-1.60 wt%	1442 (34 °C)	66	30	11.6
Au-CP-1.60 wt%	536 (154 °C)	75	73	7.2

[a] The number in brackets indicates the first reduction peak temperature.
[b] The TOFs of CO oxidation were calculated on the basis of the amount of reducible oxygen on the surface as measured by H_2-TPR; test condition: 2% CO–1% O_2–40% H_2–He; temperature: 100 °C.

TOFs at 100 °C, are given in Table 4. Of the three NM-CP catalysts (NM = Ir, Pt, Au), the Pt-CP-1.60 wt% exhibited the highest TOF value, demonstrating its highly active nature; however, such high activity also caused competitive H_2 oxidation, resulting in a dramatic decrease in selectivity to CO_2 at 180 °C. In contrast to the Pt-CP-1.60 wt% catalyst, the Au-CP-1.60 wt% catalyst yielded the best results in terms of selectivity to CO_2, while exhibiting the lowest activity for CO oxidation. These catalysts' differing performance likely is related to their different natures, with different work functions (Pt > Ir > Au) [26]. Clearly, the Ir-CP-1.60 wt% catalyst is the best choice in terms of both activity and selectivity.

Based on the foregoing discussion regarding the active sites responsible for the catalytic activity of the Ir-CP catalysts, we believe that CO oxidation could proceed via the Mars–van Krevelen mechanism [40,41]. The iridium particles embedded in the ceria matrix and interacting strongly with the ceria support could weaken the surface Ce–O bonds and facilitate the formation of more reactive oxygen [26]. In CO oxidation, the CO takes an oxygen atom from the ceria surface and creates an oxygen vacancy. The gas-phase oxygen will adsorb on the vacancies and be activated by the electron-rich environment created by the vacancies. The activated O_2 reacts with CO to form a carbonate, which decomposes to release CO_2 and heal the oxygen vacancy; thus, a catalytic cycle from CO to CO_2 is completed without direct participation of the Ir for providing CO adsorption sites.

Along with the reaction mechanism, another important point is the promoting role of H_2. In accordance with the DRIFTS study illustrated in Fig. 6, we found that the CO conversions without the presence of H_2 were significantly lower than those under the PROX conditions (Fig. 9). One of the promoting mechanisms of the oxidation of H_2 to CO may be due to the WGS reaction originating from the oxidation of H_2 to H_2O on the basis of previous reports [6,7]. Consequently, we investigated the WGS reaction over the Ir-CP-1.60 wt% catalyst using a gas composition of 2% CO and 2% H_2O balanced with He. As shown in Fig. 9, the WGS reaction began at temperatures above 140 °C, and the CO conversion was only 10% at 220 °C. Thus, we can conclude that the contribution from the WGS reaction to CO oxidation was minor in the PROX reaction, which agrees well with the effect of 5% H_2O on the PROX activity (Fig. 2). We also fed 2% H_2O to the reacting gas for CO oxidation and found that even a small amount of H_2O had a significant promotional effect on CO oxidation. In fact, the presence of H_2 and/or H_2O has been reported to enhance the rates of CO oxidation on ceria-based catalysts [9,15,21]. In this case, we tentatively attribute this promotion to the formation of bicarbonates (by reaction of carbonates with OH and/or H_2O), which decompose at a higher rate than carbonates [42,43]. Under the PROX conditions, the significant broadening above 1611 cm^{-1} may imply the formation of bicarbonate [7], as shown clearly in Fig. 6.

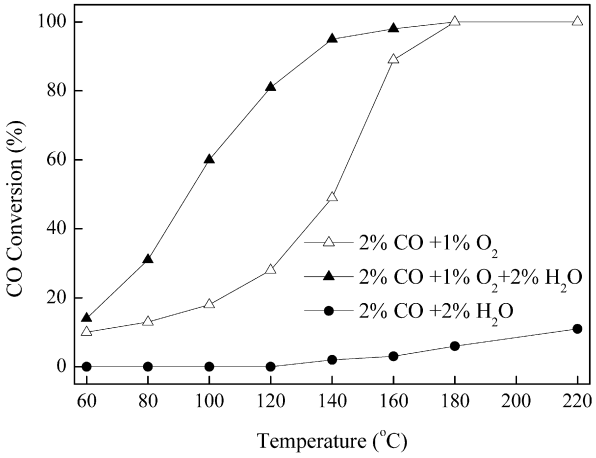

Fig. 9. CO conversion as a function of reaction temperature over the Ir-CP-1.60 wt% under different reaction conditions.

Finally, it should be kept in mind that our experimental results do not provide absolute and incontrovertible evidence of total encapsulation of the Ir species. The exposed Ir, even in a very low concentration, would contribute to the reaction through the Langmuir–Hinshelwood mechanism.

5. Conclusion

The redox-precipitation reaction between $Ir^{\delta+}$ and Ce^{3+} occurring during the CP procedure resulted in Ir particles becoming embedded in the ceria matrix. The resulting Ir-in-ceria catalyst exhibited a wide temperature window for producing a high selectivity to CO_2 and appeared to be a highly selective catalyst for the PROX reaction. The desired selectivity was probably due to the absence of extensively exposed Ir species on the ceria support, allowing suppression of hydrogen oxidation at higher temperatures. Our findings provide promising possibilities for preparing improved ceria-based catalysts for the PROX reaction.

Acknowledgments

Financial support was provided by the National Science Foundation of China (NSFC) for Distinguished Young Scholars (20325620) and NSFC grants (20673116, 20773124). The authors thank R. Prins and S.T. Oyama for help with the English and fruitful discussions.

References

[1] L. Shore, R.J. Farrauto, in: W. Vielstich, A. Lamm, H.A. Gasteiger (Eds.), Handbook of Fuel Cells: Fundamentals Technology and Applications, Part 2, vol. 3, John Wiley & Sons, West Sussex, 2003, p. 211.
[2] D.L. Trimm, Z.L. Onsan, Catal. Rev. Sci. Eng. 43 (2001) 31.
[3] D.L. Trimm, Appl. Catal. A 296 (2005) 1.
[4] S.H. Oh, R.M. Sinkevitch, J. Catal. 142 (1993) 254.
[5] F. Mariño, C. Descorme, D. Duprez, Appl. Catal. B 54 (2004) 59.
[6] A. Wootsch, C. Descorme, D. Duprez, J. Catal. 225 (2004) 259.
[7] O. Pozdnyakova, D. Teschner, A. Wootsch, J. Kröhnert, B. Steinhauer, H. Sauer, L. Toth, F.C. Jentoft, A. Knop-Gericke, Z. Paál, R. Schlögl, J. Catal. 237 (2006) 1.
[8] O. Pozdnyakova, D. Teschner, A. Wootsch, J. Kröhnert, B. Steinhauer, H. Sauer, L. Toth, F.C. Jentoft, A. Knop-Gericke, Z. Paál, R. Schlögl, J. Catal. 237 (2006) 17.
[9] O. Pozdnyakova-Tellinger, D. Teschner, J. Kröhnert, F.C. Jentoft, A. Knop-Gericke, R. Schlögl, A. Wootsch, J. Phys. Chem. C 111 (2007) 5426.
[10] D. Teschner, A. Wootsch, O. Pozdnyakova-Tellinger, J. Kröhnert, E.M. Vass, M. Hävecker, S. Zafeiratos, P. Schnörch, F.C. Jentoft, A. Knop-Gericke, R. Schlögl, J. Catal. 249 (2007) 316.
[11] C. Hardacre, R.M. Ormerod, R.M. Lambert, J. Phys. Chem. 98 (1994) 10901.
[12] S. Golunski, H. Hatcher, R. Rajaram, T. Truex, Appl. Catal. B 5 (1995) 367.
[13] S. Golunski, R. Rajaram, N. Hodge, G. Hutchings, C.J. Kiely, Catal. Today 71 (2002) 107.
[14] S. Golunski, R. Rajaram, CATTECH 6 (2002) 30.
[15] W. Deng, J.D. Jesus, H. Saltsburg, M. Flytzani-Stephanopoulos, Appl. Catal. A 291 (2005) 126.
[16] Q. Fu, H. Saltsburg, M. Flytzani-Stephanopoulos, Science 301 (2003) 935.
[17] C.M.Y. Yeung, K.M.K. Yu, Q.J. Fu, D. Thompsett, M.I. Petch, S.C.J. Tsang, J. Am. Chem. Soc. 127 (2005) 18010.
[18] C.M.Y. Yeung, F.C. Meunier, R. Burch, D. Thompsett, S.C.J. Tsang, J. Phys. Chem. B 110 (2006) 8540.
[19] R. Rajaram, J.W. Hayes, G.P. Ansell, H.A. Hatcher, U.S. patent 5,993,762, filed on 30 Nov. 1999.
[20] Y.Q. Huang, A.Q. Wang, X.D. Wang, T. Zhang, Int. J. Hydrogen Energy 32 (2007) 3880.
[21] J.L. Ayastuy, A. Gil-Rodríguez, M.P. González-Macrcos, M.A. Gutiérrez-Ortiz, Int. J. Hydrogen Energy 31 (2006) 2231.
[22] A. Trovarelli, Catal. Rev. Sci. Eng. 38 (1996) 439.
[23] A. Trovarelli (Ed.), Catalysis by Ceria and Related Materials, Imperial College Press, London, 2002, Chapter 4, p. 85.
[24] L. Tournayan, N.R. Marcilio, R. Frety, Appl. Catal. 78 (1991) 31.
[25] B. Zhang, X. Tang, Y. Li, W. Cai, Y. Xu, W. Shen, Catal. Commun. 7 (2006) 367.
[26] J.C. Frost, Nature 334 (1988) 577.
[27] Q. Fu, A. Weber, M. Flytzani-Stephanopoulos, Catal. Lett. 72 (2001) 87.
[28] A.M. Venezia, G. Pantaleo, A. Longo, G.D. Carlo, M.P. Casaletto, F.L. Liotta, G. Deganello, J. Phys. Chem. B 109 (2005) 2821.
[29] J. Guzman, S. Carrettin, J.C. Fierro-Gonzalez, Y. Hao, B.C. Gates, P. Concepción, A. Corma, Angew. Chem. Int. Ed. 44 (2005) 4778.
[30] F. Solymosi, É. Novák, A. Molnár, J. Phys. Chem. 94 (1990) 7250.
[31] A. Erdőhelyi, K. Fodor, G. Suru, Appl. Catal. A 139 (1996) 131.
[32] A. Goguet, F.C. Meunier, D. Tibiletti, J.P. Breen, R. Burch, J. Phys. Chem. B 108 (2004) 20240.
[33] C. Li, Y. Sakata, T. Arai, K. Domen, K. Maruya, T. Onishi, J. Chem. Soc. Faraday Trans. 85 (1989) 1451.
[34] A. Holmgren, B. Andersson, D. Duprez, Appl. Catal. B 22 (1999) 215.
[35] C. Milone, M. Fazio, A. Pistone, S. Galvagno, Appl. Catal. B 68 (2006) 28.
[36] F. Arena, G. Trunfio, J. Negro, B. Fazio, L. Spadaro, Chem. Mater. 19 (2007) 2269.
[37] A.J. Bard, R. Parsons, J. Jordan, in: IUPAC (Ed.), Standard Potential in Aqueous Solution, Marcel Dekker, New York, 1985, p. 617.
[38] D. Terribile, A. Trovarelli, J. Llorca, C. Leitenburg, G. Dolcetti, J. Catal. 178 (1998) 299.
[39] D. Gamarra, G. Munuera, A.B. Hungría, M. Fernández-García, J.C. Conesa, P.A. Midgley, X.Q. Wang, J.C. Hanson, J.A. Rodríguez, A. Martínez-Arias, J. Phys. Chem. C 111 (2007) 11026.
[40] P. Mars, D. Van Krevelen, Chem. Eng. Sci. (special supplement) 3 (1954) 41.
[41] V. Shapovalov, H. Metiu, J. Catal. 245 (2007) 205.
[42] M.M. Schubert, A. Venugopal, M.J. Kahlich, V. Plzak, R.J. Behm, J. Catal. 222 (2004) 32.
[43] Y. Denkwitz, Z. Zhao, U. Hörmann, U. Kaiser, V. Plzak, R.J. Behm, J. Catal. 251 (2007) 363.